AIAA JOURNAL
Vol. 46, No. 12, December 2008

Interlaminar Stresses by Sinc Method Based on Interpolation of the Highest Derivative

Wesley C. H. Slemp* and Rakesh K. Kapania†
Virginia Polytechnic Institute and State University, Blacksburg, Virginia 24060

DOI: 10.2514/1.39613

Computation of interlaminar stresses from one-dimensional equivalent-single-layer beam theories using the sinc method based on interpolation of the highest derivative is performed. The method is proposed to be an efficient tool for determining through-the-thickness variations of interlaminar stresses by the equilibrium equations of three-dimensional elasticity, because the required higher-order derivatives of displacements are accurately obtained without postprocessing, an improvement over presently used finite element methods. In functionally graded material, the sinc method offers additional benefits. Because the method employs numerical indefinite integration by double-exponential transformation, through-the-thickness integration can be performed numerically without computing additional integration weights. We obtain interlaminar stresses in symmetric cross-ply laminates and functionally graded sandwich composites using the sinc method based on interpolation of the highest derivative to approximately solve the static governing equations of the Timoshenko beam theory and the Bickford beam theory. Displacements and stresses from the present approach are compared with three-dimensional finite element method results obtained with ABAQUS/Standard. Our results indicate that the interlaminar stresses throughout the majority of the length of the beam are accurately approximated with the sinc method. The present results are significantly erroneous near the boundary because of three-dimensional edge effects not captured by the one-dimensional analysis.

I. Introduction

COMPOSITE materials remain a topic of considerable interest to researchers due to their vulnerability to impact loading. Because of interlaminar bonding imperfections, delamination can be initiated by interlaminar stresses. This effect is amplified in sandwich composites subjected to compressive loads because the face sheets tend to buckle, accentuating the risk of delamination growth. The delamination can eventually result in ultimate failure of the composite. Modern composite failure criteria incorporate the interlaminar stresses. Therefore, accurate determination of interlaminar stresses is a topic of considerable interest in the research community. We will recapitulate some of the significant developments in this area. The state of interlaminar stress computation has been reviewed extensively by Kapania and Raciti [1] and Kant and Swaminathan [2].

Interlaminar stresses may be computed directly from the constitutive equation when an exact solution is available for the three-dimensional (3-D) elasticity equations. Pagano [3] developed an exact solution for composite laminates in cylindrical bending, but there are very few specific cases in which the exact 3-D elasticity solution is available. The 3-D finite element method (FEM) has been used by many authors to determine the interlaminar stresses accurately [4]. However, the 3-D FEM is computationally expensive. Two-dimensional theories such as classical laminated plate theory (CLPT) and the first-order shear deformation theory (FSDT) provide much less expensive techniques for determining the displacements and stresses. However, CLPT assumes that there are no transverse shear strains; therefore, using the constitutive stress-strain relations alone yields no transverse shear stress components. Similarly, assuming constant transverse shear strain in FSDT results in piecewise-constant interlaminar shear strains and requires the introduction of a shear-correction factor. Higher-order theories such as Phan and Reddy's [5] consistent-third-order plate theory provide more accurate strain representations at the cost of additional computational expense.

Phan and Reddy [5] provided an alternative to the use of constitutive relations to obtain transverse normal and shear stresses by integrating the equilibrium equations of 3-D elasticity directly. However, this technique requires in-plane derivatives of in-plane strains, a feature not explicitly available from a CLPT or FSDT finite element implementation. For the transverse shear stress components, the equilibrium integration approach necessitates the first derivatives of in-plane strains. For the transverse normal stress component, the second derivatives of in-plane strains are required.

A significant amount of research has been conducted in the area of developing postprocessing schemes to be used with commercial finite element software to obtain required transverse stresses. Lajczok [6] used a finite difference scheme to compute the higher derivatives of in-plane strains necessary within the equilibrium equation approach. Byun and Kapania [7] used Chebyshev and other orthogonal polynomials to interpolate the displacements and compute the higher derivatives of in-plane strain. Lee and Lee [8] developed a postprocessing scheme for determining the transverse stresses in geometrically nonlinear composites for cross-ply symmetric composites and sandwich composites with laminated face sheets and isotropic core material. Roos et al. [9] developed a postprocessing method for determining the transverse normal stress component in doubly curved laminated shell elements in commercial finite element codes. Noor and Malik [10] used a two-stage procedure in which FSDT was used to compute in-plane stresses in stage one. In stage two, integration of the equilibrium equations of 3-D elasticity was performed to determine through-the-thickness distributions of stress. An elasticity model was used to update the in-plane stresses. Stage two was repeated until a convergence criteria on the transverse normal stress was satisfied.

In this paper, we propose a method for determining interlaminar stresses in composites using a modified sinc method based on

Presented as Paper 1750 at the 49th AIAA/ASME/ASCE/AHS/ASC Structures, Structural Dynamics, and Materials Conference, Schaumburg, IL, 7–10 April 2008; received 7 July 2008; revision received 8 September 2008; accepted for publication 8 September 2008.

*Graduate Researcher, Aerospace and Ocean Engineering, Sensors and Structural Health Monitoring Group. Student Member AIAA.

†Mitchell Professor of Aerospace Engineering, Aerospace and Ocean Engineering, Sensors and Structural Health Monitoring Group. Associate Fellow AIAA.

interpolation of the highest derivative (SIHD) [11]. Because SIHD begins with an interpolation of the highest derivative present in the governing equation, we directly obtain the necessary derivatives to determine the interlaminar stresses by integration of the equilibrium equations of 3-D elasticity. Thus, unlike schemes based on beam or plate finite elements, SIHD requires no postprocessing of displacement results to accurately obtain high-order derivatives. In this paper, we determine the transverse normal and transverse shear stresses in cross-ply symmetric laminated beams and sandwich composite beams with functionally graded core material. We extensively examine 1-D analysis of composite structures as a first step to the more general 2-D problems. We use SIHD as our computational method to solve the Timoshenko beam theory and the Bickford consistent-higher-order beam theory [12]. Through-the-thickness stress variations are compared with an approximate solution of elasticity by the finite element method implemented in ABAQUS/Standard for various thickness-to-length ratios and material configurations.

The remainder of this paper is arranged as follows: We review the SIHD for 1-D problems. We review the equivalent-single-layer (ESL) beam theories to be approximately solved by SIHD. We present a technique for determining interlaminar stresses from the displacement data by integration of the equilibrium equations of 3-D elasticity. Our results are presented and discussed for both laminated composites and sandwich composites with functionally graded core material. Finally, we provide a brief summary and our main conclusions.

II. Sinc Method Based on Interpolation of the Highest Derivative

SIHD was introduced by Li and Wu [11]. The method is an integrated collocation technique for solving elliptic two-point boundary-value problems. In the method, the highest derivative in the governing equation is approximated. Numerical double-exponential integration is used to determine the lower derivatives and the unknown function itself. Slemp and Kapania [13] suggested an alternative method for imposing the boundary conditions, which we will employ. In this section, we review some preliminary developments and describe the SIHD method.

A. Numerical Indefinite Integration Based on the Double Exponential Transform

Muhammad and Mori [14] developed a method of numerical indefinite integration based on the double-exponential (DE) transformation. The approach was used by Muhammad et al. [15] for solving integral equations by the sinc collocation method. We also refer the readers to the work of Mori [16] and Mori and Sugihara [17] for a thorough review on numerical integration using the DE transformation. We will review the concept as implemented in SIHD.

The DE transformation was proposed by Takahasi and Mori [18] in 1974 for the evaluation of integrals of analytic functions with endpoint singularities. One such DE transformation suggested by Sugihara and Matsuo [19] is

$$t = \psi(\tau) = \frac{1}{2}\tanh\left(\frac{\pi}{2}\sinh(\tau)\right) + \frac{1}{2} \tag{1}$$

The DE transformation has two salient features exploited in sinc approximate methods. First, the domain is expanded from $t \in (0, 1)$ to $\tau \in (-\infty, \infty)$. Second, the product $f(\psi(\tau))\psi'(\tau)$ decays double exponentially on the real line.

A function may be interpolated on $t \in (0, 1)$ by a sinc cardinal series exploiting the DE transformation:

$$f(t) \approx \sum_{j=-N}^{N} f(\psi(jh))\,\mathrm{sinc}\left(\frac{\phi(t)}{h} - j\right) \tag{2}$$

where $\tau = \phi(t)$ is the inverse mapping of the DE transformation, $t = \psi(\tau)$, h is the mesh size or point spacing within the $\tau \in (-\infty, \infty)$ domain, and the sinc function is defined by $\mathrm{sinc}(t) = \sin(\pi t)/(\pi t)$ for $t \neq 0$ and $\mathrm{sinc}(t) = 1$ for $t = 0$.

Consider the integration of a function $f(x)$ over the domain $(0, s)$ for any s such that $0 \leq s \leq 1$. The integrand is transformed to the $\tau \in (-\infty, \infty)$ domain, resulting in the following identity:

$$\int_0^s f(t)\mathrm{d}t = \int_{-\infty}^{\phi(s)} f(\psi(\tau))\psi'(\tau)\mathrm{d}\tau \tag{3}$$

The new integrand $f(\psi(\tau))\psi'(\tau)$ may be expanded by employing the sinc series approximation. The integration may thus be expressed as

$$\int_0^s f(t)\mathrm{d}t = h\sum_{j=-N}^{N} f(\psi(jh))\psi'(jh)\left(\frac{1}{2} + \frac{1}{\pi}\mathrm{Si}\left(\frac{\pi\phi(s)}{h} - \pi j\right)\right) \tag{4}$$

which holds for all $s \in [0, 1]$, where $\mathrm{Si}(x)$ is the sine-integral function [20] defined by

$$\mathrm{Si}\,(x) = \int_0^x \frac{\sin(s)}{s}\mathrm{d}s$$

If we consider only the discrete sinc points $s = t_i = \psi(ih)$, we may rewrite Eq. (4) at the sinc points as

$$F(t_i) = \int_0^{t_i} f(t)\mathrm{d}t = \sum_{j=-N}^{N} k_{ij} f(\psi(jh)) \tag{5}$$

where

$$k_{ij} = h\psi'(jh)(\tfrac{1}{2} + 1/\pi\mathrm{Si}[\pi(i-j)])$$

In Eq. (5), $F(t)$ represents an antiderivative of the function $f(t)$. We may repeat this process to obtain the second antiderivative of $f(t)$:

$$\int_0^{t_i} F(t)\mathrm{d}t = \sum_{j=-N}^{N}\sum_{k=-N}^{N} k_{ij}k_{jk}F(t_k) = \sum_{j=-N}^{N} g_{ij}F(t_j) \tag{6}$$

In this fashion, we may efficiently compute antiderivatives by evaluating the elements of k_{ij} and performing matrix multiplication. Also note that k_{ij} depends only on the selection of mesh size h and number of sinc points, not on the integrand. Therefore, they may easily be stored in a library and recalled for use.

B. Development of SIHD

Consider the 1-D boundary-value problem on the domain $a \leq x \leq b$:

$$L^{(m)}u(x) = s(x), \qquad a < x < b, \qquad Bu(x) = f(x), \qquad x = a, b$$

where $L^{(m)}$ is a linear differential operator of order m, and B is a linear differential operator of order less than or equal to $m - 1$.

We select $n = 2N + 1$ collocation points on $\xi \in (0, 1)$ by the DE transformation equation (1). For a mesh size h, we select collocation points corresponding to $j = \{-N, -N + 1, \ldots, N - 1, N\}$ by $\xi_j = \psi(jh)$. The domain of the boundary-value problem is transformed from $x \in [a, b]$ to $\xi \in [\xi_{-N}, \xi_N]$ by the linear transformation:

$$\xi = \frac{(\xi_N - \xi_{-N})(x - a)}{b - a} + \xi_{-N}$$

Accordingly, the boundary-value problem is rewritten in the ξ domain as

$$\tilde{L}^{(m)}\tilde{u}(\xi) = \tilde{s}(\xi), \qquad \xi_{-N} < \xi < \xi_N \tag{7}$$

$$\tilde{B}\,\tilde{u}(\xi) = \tilde{f}(\xi), \qquad \xi = \xi_{-N}, \xi_N \tag{8}$$

Assuming that we know the highest-order derivative in the governing equation $d^m\tilde{u}(\xi_j)/d\xi^m$, we may obtain an approximation

for the lower-order derivatives and the unknown function at each sinc point by Eq. (5). To that end, we write the lower derivatives and unknown function as

$$\frac{d^{m-1}\tilde{u}(\xi_i)}{d\xi^{m-1}} = k_{ij}\frac{d^m\tilde{u}(\xi_j)}{d\xi^m} + C_1$$
$$\frac{d^{m-2}\tilde{u}(\xi_i)}{d\xi^{m-2}} = k_{il}k_{lj}\frac{d^m\tilde{u}(\xi_j)}{d\xi^m} + C_1\xi_i + C_2 \quad \cdots$$
$$\frac{d\tilde{u}(\xi_i)}{d\xi} = k_{ij}^{m-1}\frac{d^m\tilde{u}(\xi_j)}{d\xi^m} + \sum_{l=1}^{m-1}\frac{C_{m-l}\xi_i^{l-1}}{(l-1)!}$$
$$\tilde{u}(\xi_i) = k_{ij}^{m}\frac{d^m\tilde{u}(\xi_j)}{d\xi^m} + \sum_{l=0}^{m-1}\frac{C_{m-l}\xi_i^{l}}{(l!)}$$

where $\{C_1, C_2, \ldots, C_m\}$ are constants of integration and a repeated index implies summation over all elements of that index.

We satisfy Eq. (7) at each of the n sinc points. The boundary-condition equation (8) is satisfied at ξ_{-N} and ξ_N to obtain a complete system of equations in terms of the unknowns:

$$\left\{C_1, C_2, \ldots, C_m, \frac{d^m\tilde{u}(\xi_j)}{d\xi^m}\right\}$$

The system is solved for these unknowns, which may be used to obtain the function $\tilde{u}(\xi_i)$ or the ith-order derivative for any i such that $1 \le i \le m$.

Implementation of SIHD for the Bickford beam problem is demonstrated in the Appendix.

III. Equivalent-Single-Layer Beam Theories

For a good overview of ESL laminated plate and beam theories, we refer to Kapania and Raciti [1], Reddy [21], and Goyal and Kapania [22]. We will review only the pertinent elements. We begin with the displacement profile of Phan and Reddy's [5] consistent-third-order plate theory:

$$U(x,y,z) = u_0(x,y) + z\phi_x(x,y) - z^3c_1\left(\phi_x(x,y) + \frac{\partial w_0}{\partial x}\right)$$
$$V(x,y,z) = v_0(x,y) + z\phi_y(x,y) - z^3c_1\left(\phi_y(x,y) + \frac{\partial w_0}{\partial y}\right)$$
$$W(x,y) = w_0(x,y)$$

where z is the rectilinear coordinate in the thickness direction, and the x–y plane of the Cartesian coordinate system is located in the midplane of the plate. The displacement field is that of Phan and Reddy's [5] third-order theory with $c_1 = 4/3h^2$, where h is the plate thickness; however, the displacement reduces to the first-order shear deformable theory by specifying $c_1 = 0$.

The infinitesimal in-plane strains of the assumed displacement field are

$$\{\epsilon\} = \{\epsilon^{(0)}\} + z\{\epsilon^{(1)}\} + z^3\{\epsilon^{(3)}\}$$

,where $\{\epsilon\} = \{\epsilon_{xx}, \epsilon_{yy}, \gamma_{xy}\}^T$. The transverse strains are $\{\gamma\} = \{\gamma^{(0)}\} + z^2\{\gamma^{(2)}\}$, where $\{\gamma\} = \{\gamma_{yz}, \gamma_{xz}\}^T$. These strains are related to the stresses by Hooke's law:

$$\{\sigma_{xx}(x,y,z), \sigma_{yy}(x,y,z), \sigma_{xy}(x,y,z)\}^T = [\bar{Q}_{ij}(z)]\{\epsilon\}(x,y,z)$$
$$\{\sigma_{yz}(x,y,z), \sigma_{xz}(x,y,z)\}^T = K[\bar{Q}_{lm}(z)]\{\gamma\}(x,y,z) \tag{9}$$

where i and j may take 1, 2, and 6; l and m may take 4 and 5; and K is the shear-correction factor. Note that K is only applicable for the FSDT or Timoshenko beam theory. For the third-order theories, we take $K = 1$.

The stress resultants are defined by

$$\{N_{\alpha\beta}, M_{\alpha\beta}, P_{\alpha\beta}\} = \int_{-h/2}^{h/2}\sigma_{\alpha\beta}\{1, z, z^3\}\mathrm{d}z$$
$$\{Q_\alpha, R_\alpha\} = K\int_{-h/2}^{h/2}\sigma_{\alpha z}\{1, z^2\}\mathrm{d}z \tag{10}$$

with α and β taking x and y. We define the stiffnesses by

$$\{A_{ij}, B_{ij}, D_{ij}, E_{ij}, F_{ij}, H_{ij}\} = \int_{-h/2}^{h/2}\bar{Q}_{ij}(z)\{1, z, z^2, z^3, z^4, z^6\}\mathrm{d}z$$
$$\{AS_{lm}, DS_{lm}, FS_{lm}\} = \int_{-h/2}^{h/2}\bar{Q}_{lm}(z)\{1, z^2, z^4\}\mathrm{d}z$$

Here, i and j may take 1, 2, and 6, and l and m may take 4 and 5. The stress resultants may be written in terms of strains by

$$\begin{Bmatrix}\{N\}\\ \{M\}\\ \{P\}\end{Bmatrix} = \begin{bmatrix}[A] & [B] & [E]\\ [B] & [D] & [F]\\ [E] & [F] & [H]\end{bmatrix}\begin{Bmatrix}\{\epsilon^{(0)}\}\\ \{\epsilon^{(1)}\}\\ \{\epsilon^{(3)}\}\end{Bmatrix}$$
$$\begin{Bmatrix}\{Q\}\\ \{R\}\end{Bmatrix} = \begin{bmatrix}[AS] & [DS]\\ [DS] & [FS]\end{bmatrix}\begin{Bmatrix}\{\gamma^{(0)}\}\\ \{\gamma^{(2)}\}\end{Bmatrix} \tag{11}$$

Beams have small width relative to the length; therefore, the stress resultants N_{yy}, N_{xy}, M_{yy}, M_{xy}, P_{xy}, P_{yy}, Q_y, and R_y vanish. The strains ϵ_{yy} and γ_{xy} are nonzero, despite differentiation with respect to y. To reduce the stress-resultant strain relations, we invert Eq. (11) and impose

$$N_{yy} = N_{xy} = M_{yy} = M_{xy} = P_{xy} = P_{yy} = Q_y = R_y = 0$$

By doing so, the strain components $\epsilon_{yy}^{(i)}$, $\gamma_{xy}^{(i)}$, and $\gamma_{yz}^{(j)}$ ($i = 0, 1, 3$ and $j = 0, 2$) are expressed in terms of $\epsilon_{xx}^{(i)}$ and $\gamma_{xz}^{(j)}$. Therefore, the stress-resultant strain relations for beams may be expressed by

$$\begin{Bmatrix}N_{xx}\\ M_{xx}\\ P_{xx}\end{Bmatrix} = \begin{bmatrix}A_{11}^* & B_{11}^* & E_{11}^*\\ B_{11}^* & D_{11}^* & F_{11}^*\\ E_{11}^* & F_{11}^* & H_{11}^*\end{bmatrix}\begin{Bmatrix}\epsilon_{xx}^{(0)}\\ \epsilon_{xx}^{(1)}\\ \epsilon_{xx}^{(3)}\end{Bmatrix}$$
$$\begin{Bmatrix}Q_x\\ R_x\end{Bmatrix} = \begin{bmatrix}AS_{55}^* & DS_{55}^*\\ DS_{55}^* & FS_{55}^*\end{bmatrix}\begin{Bmatrix}\gamma_{xz}^{(0)}\\ \gamma_{xz}^{(2)}\end{Bmatrix} \tag{12}$$

We may take a 1-D displacement field independent of y to be

$$U(x,z) = u_0(x) + z\phi_x - c_1z^3\left(\phi_x + \frac{dw_0}{dx}\right)$$

and $W(x,z) = w_0(x)$.

Our 1-D strains are

$$\epsilon_{xx}(x,z) = \epsilon_{xx}^{(0)} + z\epsilon_{xx}^{(1)} + z^3\epsilon_{xx}^{(3)}$$

and

$$\gamma_{xz}(x,z) = \gamma_{xz}^{(0)} + z^2\gamma_{xz}^{(2)}$$

with

$$\epsilon_{xx}^{(0)} = \frac{du_0}{dx}, \qquad \epsilon_{xx}^{(1)} = \frac{d\phi_x}{dx}, \qquad \epsilon_{xx}^{(3)} = -c_1\left(\frac{d\phi_x}{dx} + \frac{d^2w_0}{d^2x}\right)$$
$$\gamma_{xz}^{(0)} = \phi_x, \qquad \gamma_{xz}^{(2)} = -3c_1\left(\phi_x + \frac{dw_0}{dx}\right) \tag{13}$$

Because we consider only symmetric beams, we may take $u_0 = 0$, and thus the bending and extensional equations uncouple.

The governing equations and boundary conditions for the Timoshenko beam are provided by Reddy [21]. The governing equations for the Bickford beam are summarized in the Appendix. An approximate solution of the governing equations and the pertinent boundary conditions is found using SIHD, as described in

Sec. II. We demonstrate how SIHD is implemented for the Bickford beam in the Appendix.

With our approximate solution [$w(x)$, $\phi(x)$, and their derivatives], the 2-D strains are found for stress computation in the following manner: The stress resultants $N_{\alpha\beta}$, $M_{\alpha\beta}$, and $P_{\alpha\beta}$ ($\alpha, \beta = x, y$) are calculated from the 1-D strains according to Eq. (12). The in-plane 2-D strains $\{\epsilon^{(0)}\}$, $\{\epsilon^{(1)}\}$, and $\{\epsilon^{(3)}\}$ are determined by inverting Eq. (11).

IV. Transverse Shear and Transverse Normal Stress Components

The transverse shear and transverse normal stress components may be computed by integrating the equilibrium equations of 3-D elasticity. The equilibrium equations, neglecting the effects of in-plane stresses on the z-direction equilibrium and with no body forces, are given by $\sigma_{\alpha\beta,\beta} = 0$, where α and β may take x, y, and z. We may extract the transverse normal and transverse shear terms by integrating with respect to z to obtain

$$\sigma_{xz}(x, s) - \sigma_{xz}(x, z_0) = -\int_{z_0}^{s}\left(\frac{\partial\sigma_{xx}}{\partial x} + \frac{\partial\sigma_{xy}}{\partial y}\right)\mathrm{d}z \tag{14}$$

$$\sigma_{yz}(x, s) - \sigma_{yz}(x, z_0) = -\int_{z_0}^{s}\left(\frac{\partial\sigma_{xy}}{\partial x} + \frac{\partial\sigma_{yy}}{\partial y}\right)\mathrm{d}z \tag{15}$$

$$\sigma_{zz}(x, s) - \sigma_{zz}(x, z_0) = -\int_{z_0}^{s}\left(\frac{\partial\sigma_{xz}}{\partial x} + \frac{\partial\sigma_{yz}}{\partial y}\right)\mathrm{d}z \tag{16}$$

Given first-order in-plane derivatives of in-plane stresses, we may integrate to obtain the transverse shear stress components at some arbitrary thickness position s relative to the value at some z_0. With second-order in-plane derivatives of in-plane stresses, we may compute the transverse normal stress component.

A. Laminated Composites

Consider a laminated composite beam for which the geometry may be seen in Fig. 1. For such a beam, the stiffnesses vary only across layer boundaries, and thus the integration may be performed on a layer-by-layer basis in an analytic fashion.

In this paper, we consider only 1-D problems; therefore, derivatives with respect to y vanish in the elasticity equations. We assume third-order in-plane strains, consistent with the Bickford theory. The constitutive law equation (9) is substituted into the transverse shear stress component equations to obtain

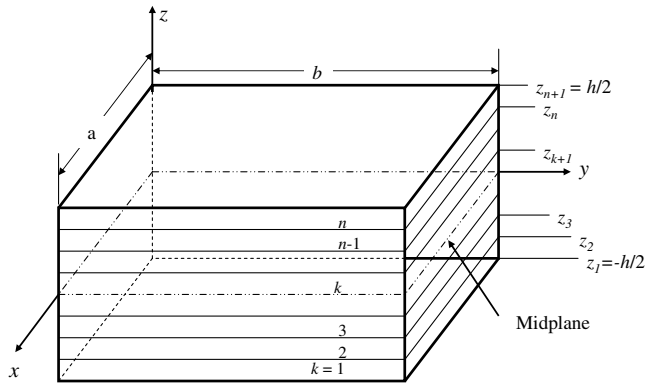

Fig. 1 Geometry of a laminated composite plate.

$$\begin{aligned}\sigma_{xz}(x, s) - \sigma_{xz}(x, z_k) &= -\int_{z_k}^{s}\Big(\{\bar{Q}_{1j}\}^{(k)}\frac{d\{\epsilon^{(0)}\}}{dx} \\ &\quad + z\{\bar{Q}_{1j}\}^{(k)}\frac{d\{\epsilon^{(1)}\}}{dx} + z^3\{\bar{Q}_{1j}\}^{(k)}\frac{d\{\epsilon^{(3)}\}}{dx}\Big)\mathrm{d}z \\ \sigma_{yz}(x, s) - \sigma_{yz}(x, z_k) &= -\int_{z_k}^{s}\Big(\{\bar{Q}_{6j}\}^{(k)}\frac{d\{\epsilon^{(0)}\}}{dx} \\ &\quad + z\{\bar{Q}_{6j}\}^{(k)}\frac{d\{\epsilon^{(1)}\}}{dx} + z^3\{\bar{Q}_{6j}\}^{(k)}\frac{d\{\epsilon^{(3)}\}}{dx}\Big)\mathrm{d}z\end{aligned} \tag{17}$$

where $\{\bar{Q}_{1j}\} = \{\bar{Q}_{11}, \bar{Q}_{12}, \bar{Q}_{16}\}$, $\{\bar{Q}_{6j}\} = \{\bar{Q}_{16}, \bar{Q}_{26}, \bar{Q}_{66}\}$, and s is an arbitrary thickness location such that $z_k \le s \le z_{k+1}$. The integration may be performed analytically to obtain

$$\begin{aligned}\sigma_{xz}(x, s) - \sigma_{xz}(x, z_k) &= -(s - z_k)\{\bar{Q}_{1j}\}^{(k)}\frac{d\{\epsilon^{(0)}\}}{dx} \\ &\quad - \frac{(s^2 - z_k^2)}{2}\{\bar{Q}_{1j}\}^{(k)}\frac{d\{\epsilon^{(1)}\}}{dx} - \frac{(s^4 - z_k^4)}{4}\{\bar{Q}_{1j}\}^{(k)}\frac{d\{\epsilon^{(3)}\}}{dx}\end{aligned}$$

and a similar expression for σ_{yz}.

A piecewise expression for $d\sigma_{xz}/dx$ may be obtained by differentiating the preceding expression with respect to x. Thus, we may analytically perform the integration in Eq. (16). Accordingly, we write the transverse normal stress variation to be

$$\begin{aligned}\sigma_{zz}(x, s) - \sigma_{zz}(x, z_k) &= -\frac{d\sigma_{xz}(x, z_k)}{dx}(s - z_k) \\ &\quad + \left(\frac{(s^2 - z_k^2)}{2} - z_k(s - z_k)\right)\{\bar{Q}_{1j}\}^{(k)}\frac{d\{\epsilon^{(0)}\}}{dx} \\ &\quad + \left(\frac{(s^3 - z_k^3)}{6} - \frac{z_k^2(s - z_k)}{2}\right)\{\bar{Q}_{1j}\}^{(k)}\frac{d\{\epsilon^{(1)}\}}{dx} \\ &\quad + \left(\frac{(s^5 - z_k^5)}{20} - \frac{z_k^4(s - z_k)}{4}\right)\{\bar{Q}_{1j}\}^{(k)}\frac{d\{\epsilon^{(3)}\}}{dx}\end{aligned}$$

The terms $\sigma_{xz}(x, z_k)$, $d\sigma_{xz}(x, z_k)/dx$, and $\sigma_{zz}(x, z_k)$ are computed for $k = 1$, taking the bottom surface to be free from stress. This implies

$$\sigma_{xz}(x, z_1) = \frac{d\sigma_{xz}(x, z_1)}{dx} = \sigma_{zz}(x, z_1) = 0$$

For $k > 1$, we equate the tractions between layers:

$$\sigma_{xz}(x, z_k) = \sigma_{xz}(x, z_{k-1})$$

$$\sigma_{zz}(x, z_k) = \sigma_{zz}(x, z_{k-1})$$

This condition implies

$$\frac{d\sigma_{xz}(x, z_k)}{dx} = \frac{d\sigma_{xz}(x, z_{k-1})}{dx}$$

It should be noted that the transverse shear stress may be computed by the constitutive equation for the Bickford and Timoshenko beam theories. Accordingly, the tractions would not be equal across layer boundaries:

$$\sigma_{xz}(x, z_k) \neq \sigma_{xz}(x, z_{k-1}), \qquad \sigma_{zz}(x, z_k) \neq \sigma_{zz}(x, z_{k-1})$$

However, we choose to ignore the constitutive equations for these cases and impose the more accurate elasticity boundary conditions

$$\sigma_{xz}(x, z_k) = \sigma_{xz}(x, z_{k-1}), \qquad \sigma_{zz}(x, z_k) = \sigma_{zz}(x, z_{k-1})$$

B. Functionally Graded Sandwich Composites

Consider a sandwich plate with isotropic face sheets and a functionally graded core, as shown in Fig. 2. The core has varying volume fractions of two constituent materials. There are several

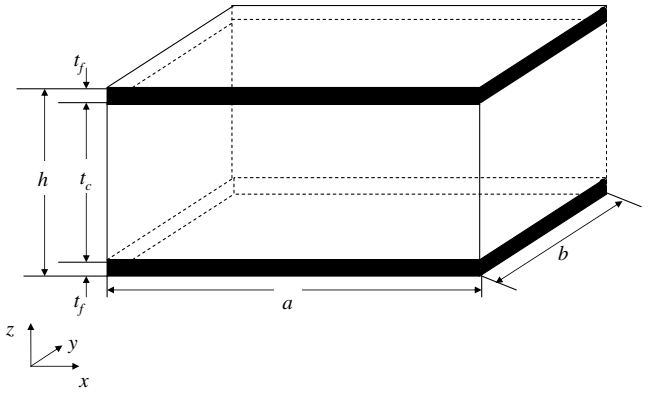

Fig. 2 Geometry of a functionally graded plate.

methods for homogenization of a multiconstituent material. Both the rule-of-mixtures approach and Mori–Tanaka [23] methods have been used in conjunction with functionally graded materials [24–26]. We use the Mori–Tanaka [23] approach. Accordingly, the material properties may be determined by

$$\frac{K-K_1}{K_2-K_1}=\frac{V_2}{1+(1-V_2)(K_2-K_1)/(K_1+4/3G_1)}$$

$$\frac{G-G_1}{G_2-G_1}=\frac{V_2}{1+(1-V_2)[(G_2-G_1)/(G_1+f_1)]}$$

$$f_1=\frac{G_1(9K_1+8G_1)}{6(K_1+2G_1)}$$

where K, K_1, and K_2 are the bulk moduli of the homogenized material, constituent 1, and constituent 2, respectively, and G, G_1, and G_2 are the shear moduli of the homogenized material, constituent 1, and constituent 2, respectively. The effective values of Young's modulus and Poisson's ratio are found from the bulk and shear moduli. The plane-stress reduced-stiffness matrix $[\bar{Q}(z)]$ is known, having obtained the homogenized engineering constants.

It is clear from the homogenization method that analytic integration through the core is not practical. Through the face sheets, $-h/2 \le z \le -h/2+t_f$ and $h/2-t_f \le z \le h/2$, the integration may be performed in an identical fashion to laminated composites. However, for the core we will use the numerical indefinite integration using double-exponential transformation. We write Eq. (17), integrating through the core with $z_0=-h/2+t_f$ for s such that $(-h/2+t_f) \le s \le (h/2-t_f)$. To compute the transverse shear stress components, we must evaluate

$$\int_{z_0}^{s}\{\bar{Q}(z)\}\mathrm{d}z, \qquad \int_{z_0}^{s} z\{\bar{Q}(z)\}\mathrm{d}z, \qquad \int_{z_0}^{s} z^3\{\bar{Q}(z)\}\mathrm{d}z$$

To do so, we change the domain from $z \in (-h/2+t_f, h/2-f_f)$ to $\xi \in (0, \xi_N)$ by the transformation $z=(\xi)(h-2t_f)/\xi_N - h/2 + t_f$. Accordingly, we must evaluate

$$\int_0^{\xi_j}\{\bar{Q}(z(\xi))\}\frac{dz}{d\xi}\mathrm{d}\xi, \qquad \int_0^{\xi_j} z(\xi)\{\bar{Q}(z(\xi))\}\frac{dz}{d\xi}\mathrm{d}\xi$$

$$\int_0^{\xi_j} z^3(\xi)\{\bar{Q}(z(\xi))\}\frac{dz}{d\xi}\mathrm{d}\xi$$

Applying Eq. (5), we obtain

$$\int_0^{\xi_j}\{\bar{Q}(z(\xi))\}\frac{dz}{d\xi}\mathrm{d}\xi \approx \sum_{i=-N}^{N}\frac{dz}{d\xi}k_{ji}\{\bar{Q}(z(\xi_i))\}$$

$$\int_0^{\xi_j} z(\xi)\{\bar{Q}(z(\xi))\}\frac{dz}{d\xi}\mathrm{d}\xi \approx \sum_{i=-N}^{N}\frac{dz}{d\xi}k_{ji}z(\xi_i)\{\bar{Q}(z(\xi_i))\}$$

$$\int_0^{\xi_j} z^3(\xi)\{\bar{Q}(z(\xi))\}\frac{dz}{d\xi}\mathrm{d}\xi \approx \sum_{i=-N}^{N}\frac{dz}{d\xi}k_{ji}z^3(\xi_i)\{\bar{Q}(z(\xi_i))\}$$

Note that k_{ij} was already computed to obtain an approximate solution to our boundary-value problem by SIHD. Thus, *the transverse shear stress components may be obtained without significant additional computational expense*.

The transverse shear stress for a functionally graded material is approximated by

$$\sigma_{xz}(x,z(\xi_l))-\sigma_{xz}(x,z_0)=-\sum_{i=-N}^{N}k_{li}\frac{dz}{d\xi}\left(\{\bar{Q}_{1j}(z(\xi_i))\}\frac{d\{\epsilon^{(0)}\}}{dx}+z(\xi_i)\{\bar{Q}_{1j}(z(\xi_i))\}\frac{d\{\epsilon^{(1)}\}}{dx}+z^3(\xi_i)\{\bar{Q}_{1j}(z(\xi_i))\}\frac{d\{\epsilon^{(3)}\}}{dx}\right) \tag{18}$$

with $z_0=-h/2+t_f$ for all sinc points $z(\xi_l) \in (-h/2+t_f, h/2-t_f)$. A similar expression may be obtained for $\sigma_{yz}(x,z(\xi_l))$. The transverse normal stress distribution through the thickness is obtained in a similar manner. By equilibrium, the transverse normal stress may be obtained as

$$\sigma_{zz}(x,s)-\sigma_{zz}(x,z_0)=-\int_{z_0}^{s}\left(-\int_{z_0}^{s_1}\left(\{\bar{Q}_{1j}(z)\}\frac{d^2\{\epsilon^{(0)}\}}{dx^2}+z\{\bar{Q}_{1j}(z)\}\frac{d^2\{\epsilon^{(1)}\}}{dx^2}+z^3\{\bar{Q}_{1j}(z)\}\frac{d^2\{\epsilon^{(3)}\}}{dx^2}\right)\mathrm{d}z+\frac{\partial\sigma_{xz}(x,z_0)}{\partial x}\right)\mathrm{d}s_1 \tag{19}$$

To evaluate Eq. (19), we must obtain

$$\int_{z_0}^{s}\int_{z_0}^{s_1}\{\bar{Q}(z)\}\mathrm{d}z\mathrm{d}s_1, \qquad \int_{z_0}^{s}\int_{z_0}^{s_1} z\{\bar{Q}(z)\}\mathrm{d}z\mathrm{d}s_1$$

$$\int_{z_0}^{s}\int_{z_0}^{s_1} z^3\{\bar{Q}(z)\}\mathrm{d}z\mathrm{d}s_1$$

To do so, the domain is again transformed from $z \in (-h/2+t_f, h/2-f_f)$ to $\xi \in (0, \xi_N)$. Now we apply the double-exponential integration scheme in Eq. (6) to evaluate these integrals at each sinc point. The transverse normal stress for a functionally graded material is approximated by

$$\sigma_{zz}(x,z(\xi_l))-\sigma_{zz}(x,z_0)=-\sum_{m=-N}^{N}\sum_{i=-N}^{N}k_{lm}k_{mi}\left(\frac{dz}{d\xi}\right)^2\left(-\left(\{\bar{Q}_{1j}(z(\xi_i))\}\frac{d^2\{\epsilon^{(0)}\}}{dx^2}+z(\xi_i)\{\bar{Q}_{1j}(z(\xi_i))\}\frac{d^2\{\epsilon^{(1)}\}}{dx^2}+z^3(\xi_i)\{\bar{Q}_{1j}(z(\xi_i))\}\frac{d^2\{\epsilon^{(3)}\}}{dx^2}\right)\right)-\frac{\partial\sigma_{xz}(x,z_0)}{\partial x}(z(\xi_i)-z_0) \tag{20}$$

Once again, we emphasize that because we use SIHD, k_{ij} is evaluated to obtain our approximate solution to the boundary-value problem. Therefore, obtaining the transverse normal and transverse shear stress components from the elasticity equations is simply reduced to matrix multiplication.

V. Results and Discussion

The bending of symmetric composite beams was examined using the 3-D FEM and the ESL beam theories solved by SIHD. Both cross-ply laminated composite beams and beams with isotropic face sheets and functionally graded core material were considered. The beams were subjected to static uniform transverse loading. The displacements and stresses, including transverse normal and transverse shear stress components computed by integration of the equilibrium equations of elasticity, were compared with an approximate elasticity solution using the conventional 3-D FEM. To our knowledge, there is no exact elasticity solution for this type of beam. All stress and displacement results were normalized in the following manner:

Table 1 Three-dimensional finite element mesh size for laminated beams

a/h	Length	Height	Width
5	140[a]	49[b]	26
10	140[a]	42[c]	26
20	240[a]	38[c]	26

[a]Elements spacing is biased toward the beam ends with a bias ratio of 5.
[b]Element spacing is biased in both 0 deg laminate layers with a bias ratio of 5.
[c]Element spacing is biased in the top 0 deg laminate layer with a bias ratio of 5.

$$\bar{\sigma}_{xx} = \sigma_{xx}h^2/a^2p_0, \qquad \bar{\sigma}_{xz} = \sigma_{xz}h/ap_0$$
$$\bar{\sigma}_{zz} = \sigma_{zz}/p_0, \qquad \bar{w} = wE_1h^3/p_0a^4$$

where h is the beam thickness, a is the beam length, and p_0 is the magnitude of the applied load.

A. Laminated Beams

Three-layered (0/90/0) graphite/epoxy laminates were considered. Beams with length-to-thickness a/h ratios of 5, 10, and 20 and a slenderness ratio equal to the length-to-thickness ratio ($a/b = a/h$) were examined. For each case, numerical results were obtained using SIHD with both the Timoshenko beam theory and Bickford's consistent-higher-order beam theory. The following material properties for a typical orthotropic graphite/epoxy lamina [7] were used for the laminated beams:

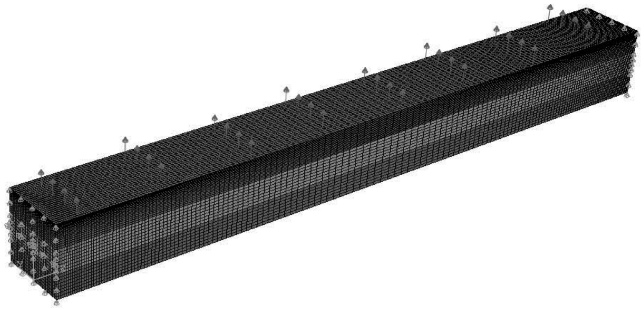

Fig. 3 Three-dimensional FEM for 0/90/0 graphite/epoxy laminated composite beam.

$$E_1 = 1.72 \times 10^{11}\ \text{N/m}^2, \qquad E_2 = E_3 = 6.89 \times 10^9\ \text{N/m}^2$$
$$G_{12} = 3.45 \times 10^9\ \text{N/m}^2, \qquad G_{13} = G_{23} = 1.38 \times 10^9\ \text{N/m}^2$$
$$\nu_{12} = \nu_{13} = \nu_{23} = 0.25$$

Eight-node linear reduced-integration brick elements (C3-D8R) in ABAQUS/Standard were used to obtain an approximate elasticity solution for each length-to-thickness ratio. The beam's thickness was maintained while we increased the length of the beam to vary a/h (a/b maintained). We reduced the element size until we obtained a similar solution from two successively fine meshes. The converged mesh sizes are summarized in Table 1. The simply supported boundary condition was enforced at both edges by constraining all nodes on the transverse faces from w translation. The midplane's

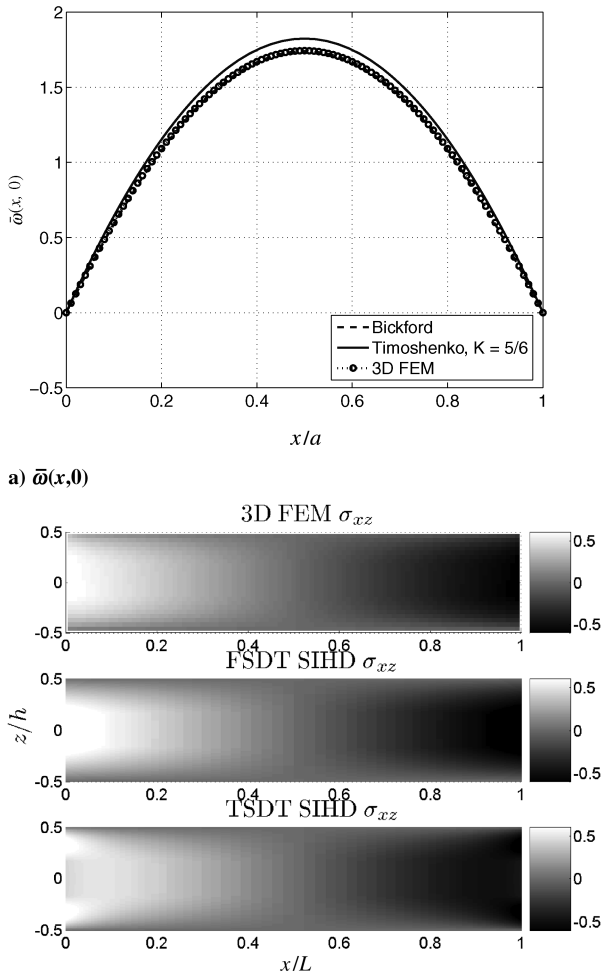

a) $\bar{\omega}(x,0)$ c) $\bar{\sigma}_{xz}(x,z)$

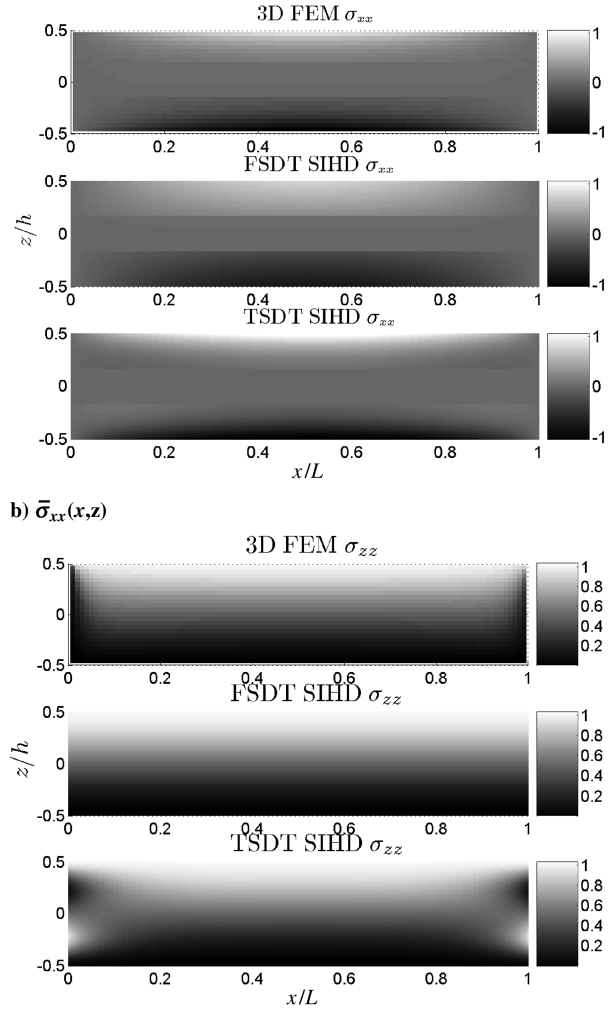

b) $\bar{\sigma}_{xx}(x,z)$ d) $\bar{\sigma}_{zz}(x,z)$

Fig. 4 Fringe plots of stress components in a simply supported laminated beam with $a/h = 5$.

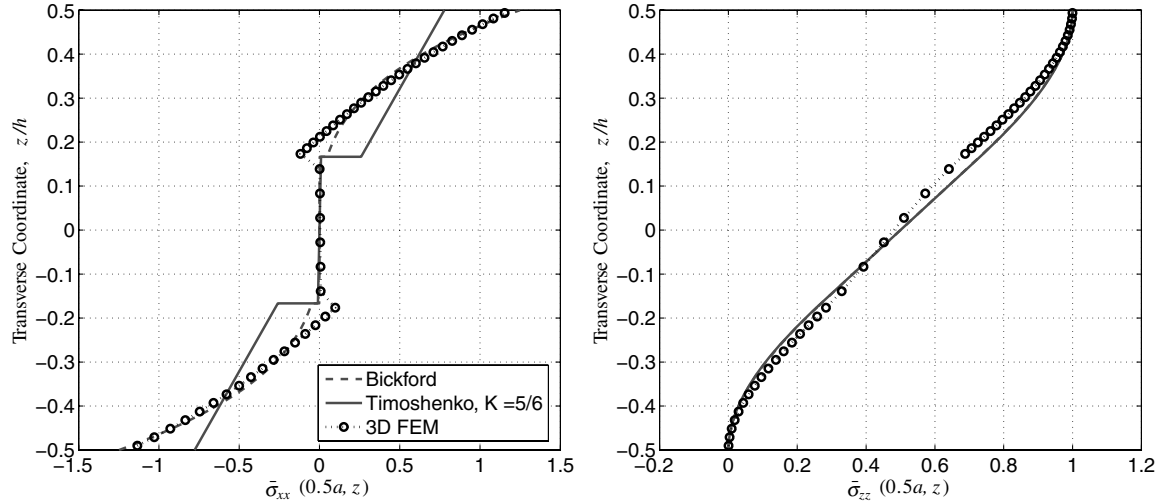

Fig. 5 Longitudinal and transverse normal stress components at the beam center for a simply supported laminated beam with $a/h = 5$.

intersection with the $x = 0$ transverse face was constrained in the x direction, allowing Poisson contraction in the x direction. The central node on a transverse edge was constrained against v translation, preventing a rigid-body mode while allowing Poisson contraction in the y direction. The 3-D FEM mesh for a laminated beam, with $a/h = 10$ and with boundary conditions and loading indicated, may be seen in Fig. 3.

The present results were obtained using SIHD implemented in MATLAB R14 service pack 2. For our SIHD results, we use $N = 100$ (201 sinc points) in the original sinc approximation in Eq. (2). This choice guarantees convergence at the cost of a nearly undetectable computation time, on the order of 0.5 s on a typical dual-processor PC. The sinc mesh size h [see Eq. (2)] was taken as $2.5/N$ [13].

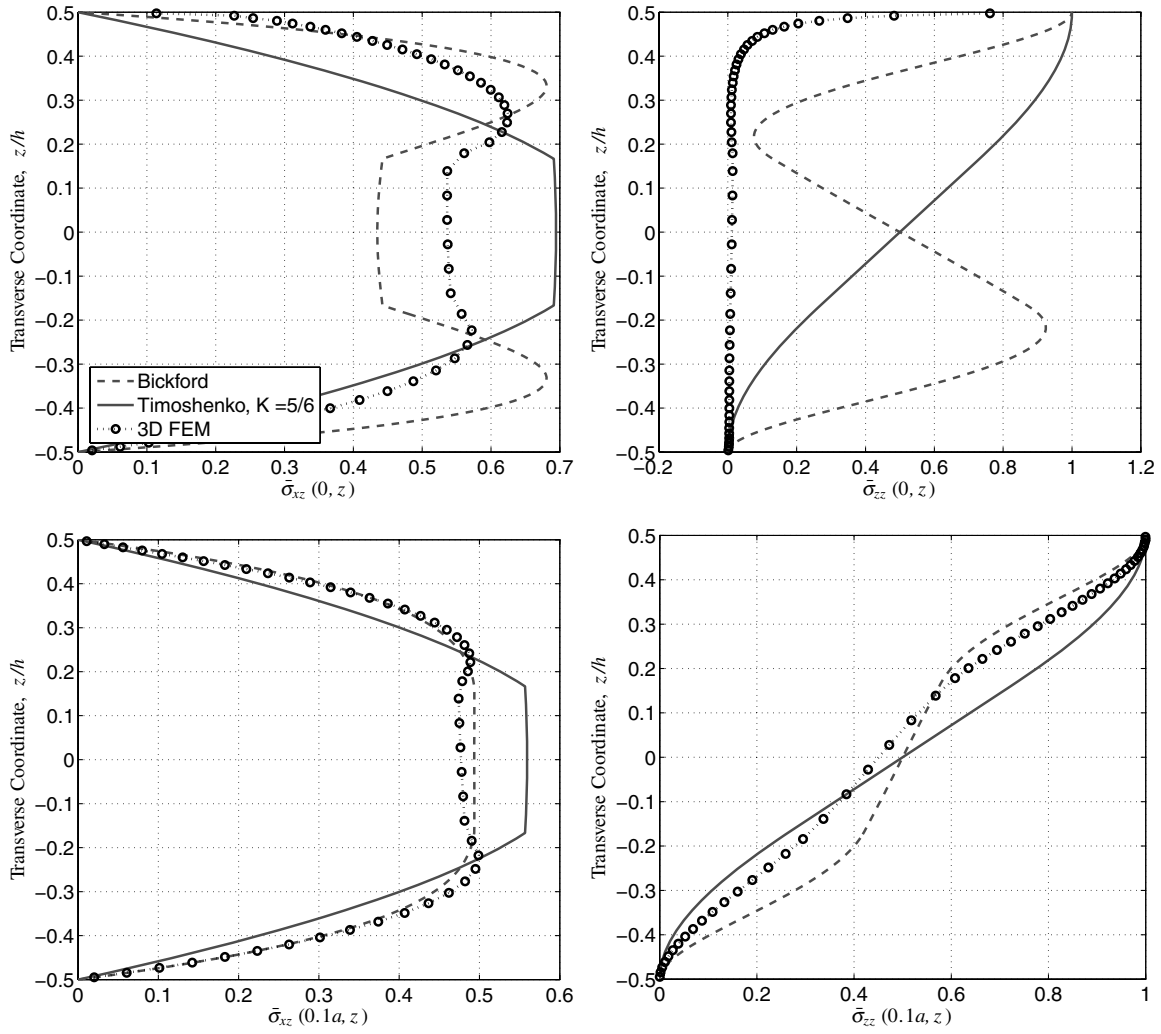

Fig. 6 Longitudinal and transverse normal stress components at $x = 0, 0.1a$ for a simply supported laminated beam with $a/h = 5$.

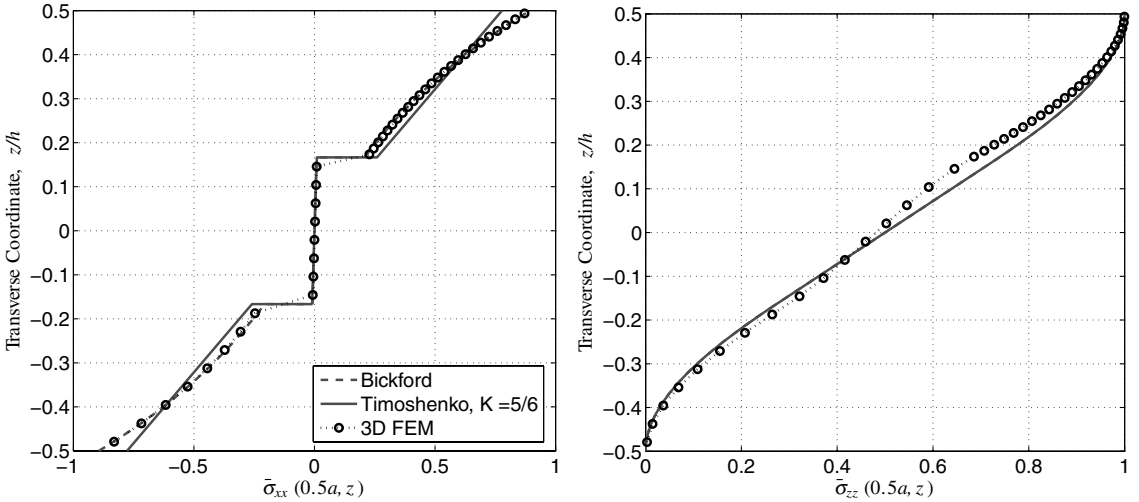

Fig. 7 Longitudinal and transverse normal stress components at the beam center for a simply supported laminated beam with $a/h = 10$.

In Fig. 4, we plot the displacement of the midplane and fringe plots of through-the-thickness midplane ($y = 0$) stresses for $a/h = 5$. The figure indicates that the displacements are very accurately computed using the Bickford theory. Figure 4b indicates that the trend of σ_{xx} is captured very well by the Timoshenko theory (FSDT) and the Bickford or third-order shear deformable theory (TSDT). Figure 4c indicates that the trend of σ_{xz} is captured by both theories for most of the beam; however, the Bickford theory appears to differ significantly from the FEM results in the vicinity of the boundary. Figure 4d also indicates that the trend of σ_{zz} is not well captured in the vicinity of the boundaries. Neither the Timoshenko theory nor the Bickford theory fully capture the transverse normal stress component in these areas.

Through-the-thickness stress distributions are plotted in Figs. 5 and 6. The longitudinal normal stress component σ_{xx} is plotted at the midpoint of the beam in Fig. 5. The figure indicates that the stress

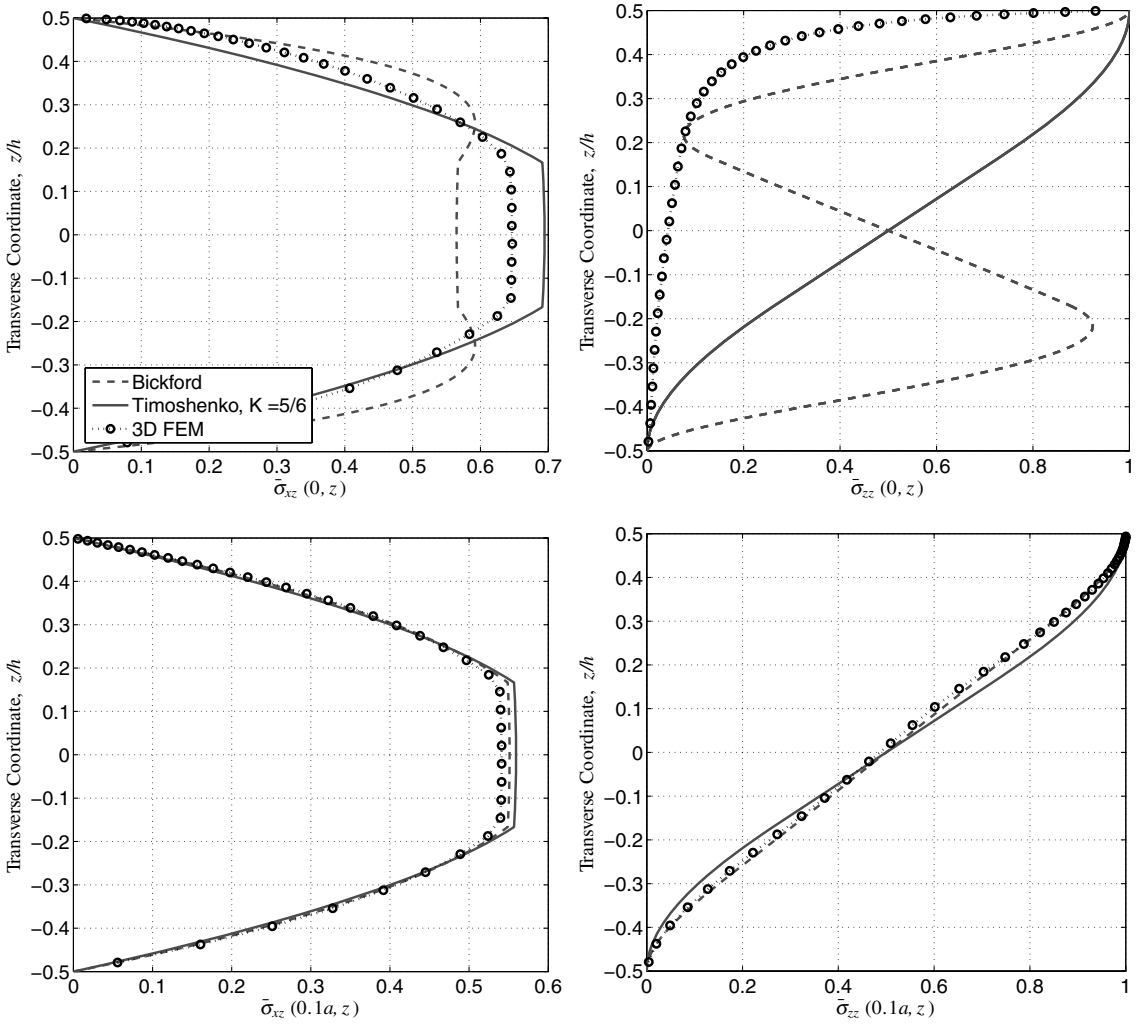

Fig. 8 Longitudinal and transverse normal stress components at $x = 0, 0.1a$ for a simply supported laminated beam with $a/h = 10$.

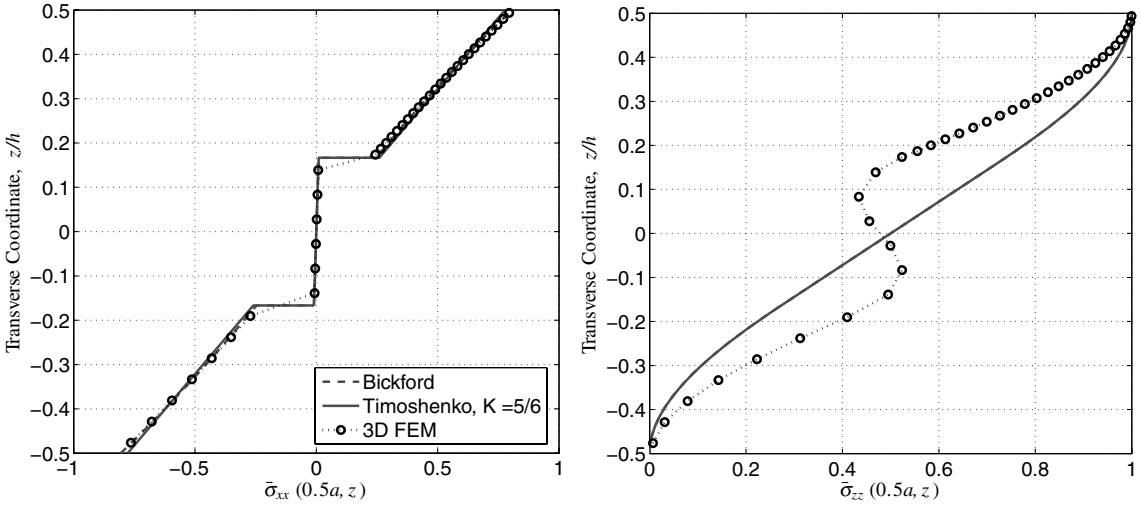

Fig. 9 Longitudinal and transverse normal stress components at the beam center for a simply supported laminated beam with $a/h = 20$.

distribution is very accurately predicted by the Bickford theory. However, the Timoshenko theory fails to capture the trend precisely. This result is due to the higher-order of the assumed displacements in the Bickford theory making it beneficial for studying thick beams such as $a/h = 5$. The transverse normal stress component is also plotted in Fig. 5. At the midpoint, we see that the transverse normal stress component for this beam is very accurately predicted by both of the theories.

In Fig. 6, we plotted through-the-thickness stress distributions of transverse shear (σ_{xz}) and transverse normal (σ_{zz}) stresses at the end ($x/a = 0$) and near the end ($x/a = 0.1$) of the beam. The figures indicate erroneous stresses computed by the ESL theories in the vicinity of the edge. The Bickford theory captures the trend of transverse shear stress at $x = 0$; however, the peak stress in the 0 deg layers is reported to be higher than the 3-D FEM. The transverse normal stress component computed by the ESL theories differs

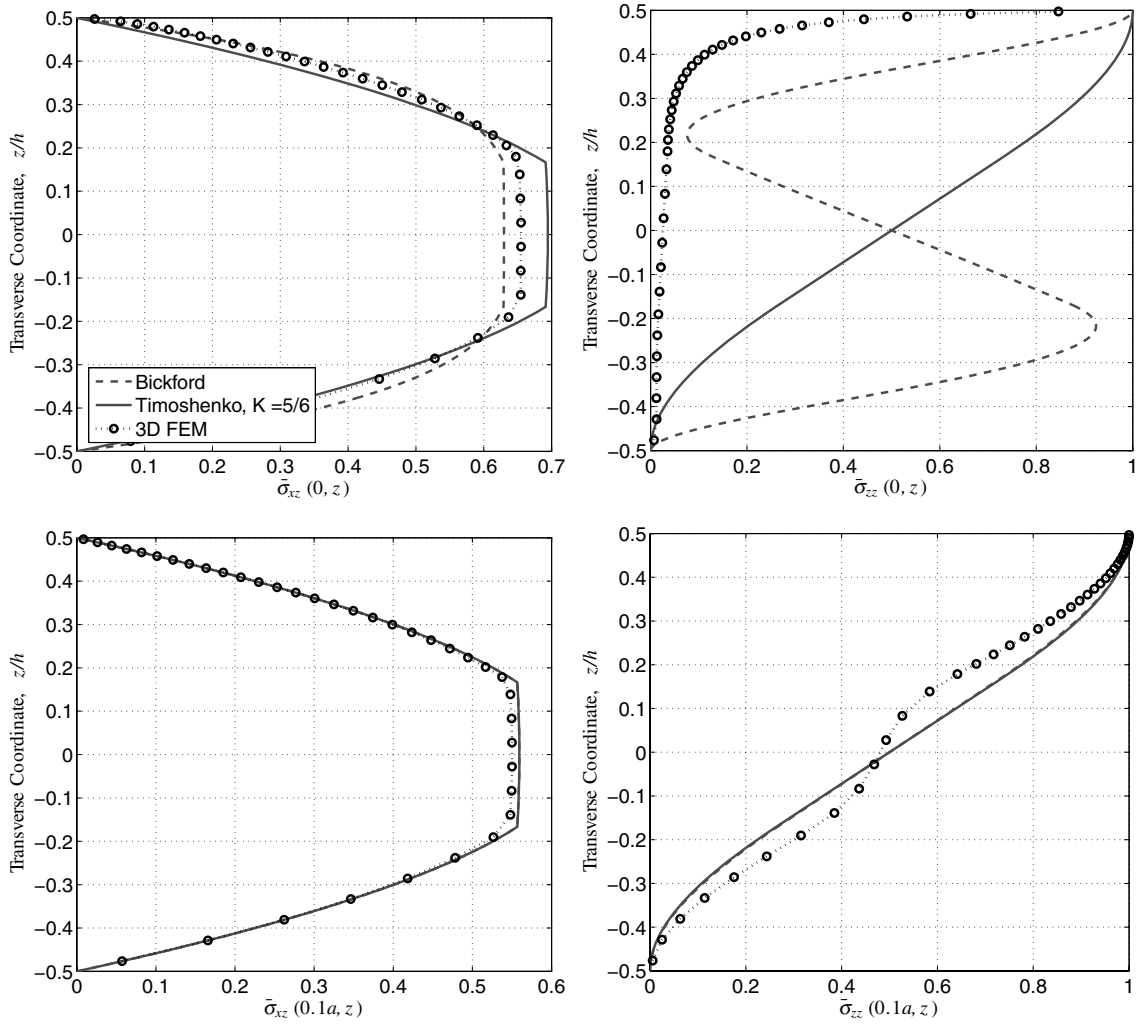

Fig. 10 Longitudinal and transverse normal stress components at $x = 0, 0.1a$ for a simply supported laminated beam with $a/h = 20$.

Table 2 Three-dimensional finite element mesh size for a functionally graded core

p	Length	Height	Width
1	140[a]	34[b]	14
2	140[a]	34[b]	14
∞	140[a]	34[b]	14

[a]Elements spacing is biased toward beam ends with a bias ratio of 5.
[b]Elements spacing in the face sheets biased toward top and bottom surfaces with a bias ratio of 5.

significantly from the FEM at $x/a = 0$. However, we note the inaccuracies of the finite element solution in this vicinity as well. The 3-D FEM results for transverse normal stress only approximately achieve the applied load on the top surface. Significant further refinement is necessary to precisely obtain the boundary condition at an additional cost to an already expensive analysis. However, it is safe to assume that the present results obtained by the ESL theories are also inaccurate because of the failure to capture the trend of the FEM results. In this area, the relative dimensions of thickness and width are both on the same scale as the distance from the end. Thus, the error seen at $x/a = 0$ is likely due to 3-D effects that cannot be predicted by the 1-D analysis. Nonetheless, the present results compare well with 3-D FEM at $x/a = 0.1$. The transverse shear stress component is very accurately computed by the Bickford theory. Both ESL theories compare well with 3-D FEM for transverse normal stress.

Through-the-thickness stress distributions were plotted in Figs. 7 and 8 for $a/h = 10$. The longitudinal normal stress component σ_{xx} is plotted at the midpoint of the beam in Fig. 7. The figure indicates that the stress distribution is very accurately predicted by both ESL theories. However, the Bickford theory more accurately predicts the longitudinal stress, compared with the 3-D FEM. The transverse normal stress component is also plotted in Fig. 7; both ESL theories accurately predict this distribution.

In Fig. 8, we have plotted through-the-thickness stress distributions of transverse shear and transverse normal stress at the end ($x/a = 0$) and near the end ($x/a = 0.1$) of the beam. The results are similar to the thick beam ($a/h = 5$). The ESL theories fail to predict the stresses in the vicinity of the boundary; however, the error is contained only within a small region around the boundary and improves significantly outside this region. At $x/a = 0.1$, both stress components are very accurately computed.

In Figs. 9 and 10, through-the-thickness stress distributions of longitudinal, transverse shear, and transverse normal stress components are plotted at the midpoint and near the end of the beam ($x/a = 0.5, 0, 0.1$). Other than at $x/a = 0$, the results from the Timoshenko theory and Bickford theory are indistinguishable. This indicates that there is no benefit of using the higher-order Bickford theory for thin beams. Furthermore, Fig. 10 echoes our previous comments regarding the erroneous stress at the boundary. Although neither σ_{xz} nor σ_{zz} are accurately computed at the boundary, both ESL theories compare well with the 3-D FEM at $x/a = 0.1$.

The plots of through-the-thickness stress variation implicitly indicate the relative magnitude of the stresses. The stresses σ_{xx}, σ_{xz}, and σ_{zz} were normalized by $(a/h)^2 p_0$, $(a/h)p_0$, and p_0, respectively. Note that the maximum $\bar{\sigma}_{xx}$, $\bar{\sigma}_{xz}$, and $\bar{\sigma}_{zz}$ from the fringe plots for $a/h = 5$ are approximately 1, 0.5, and 1, respectively. Thus, the relative magnitude of $\sigma_{xx}/\sigma_{xz} \approx 2a/h$ and $\sigma_{xx}/\sigma_{zz} \approx (a/h)^2$. It is reasonable to conclude for thin beams that σ_{xx} is large relative to the other stress components and that the inaccuracies of the transverse shear and transverse normal stresses may be negligible compared with the magnitude of the longitudinal bending stress.

For both $a/h = 10$ and 20, the deflection at the midplane was very accurately computed using both ESL theories. We omit these results for the sake of brevity. We also considered clamped–free beams. The results also confirm the inability of the SIHD implementation of the ESL theories to obtain accurate stresses at the boundary. Through-the-thickness distributions of transverse normal stress at both the clamped and free ends differed significantly from the 3-D FEM results.

B. Functionally Graded Sandwich Composites

Sandwich composites with a functionally graded core were also considered. The core material properties were composed of two constituent materials: a lightweight material with relatively low stiffness and the high-stiffness face-sheet material. The volume fraction varies through the core, providing smooth material-property variation from point to point. We considered the variation of volume fraction through the core of the form $V_1 = |2z/t_c|^p$ for $-t_c/2 \le z \le t_c/2$, where t_c is the core thickness, V_1 is the volume fraction of the face-sheet material, and p is the order of the polynomial variation. We considered $p = 1$, 2, and ∞.

We consider isotropic constituent materials. We used $E = 7.0 \times 10^{10}$ N/m^2 and $\nu = 0.3$ for the face-sheet material, and we take

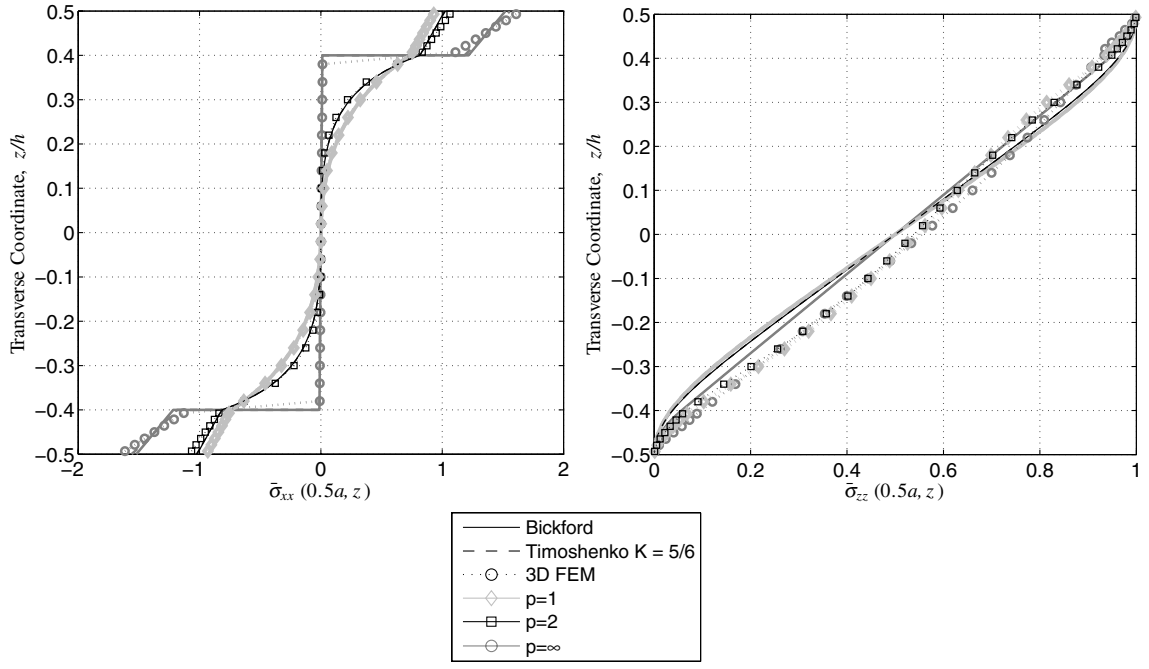

Fig. 11 Longitudinal and transverse normal stress components at the beam center for a functionally graded sandwich beam with $p = 1, 2, 4, \infty$.

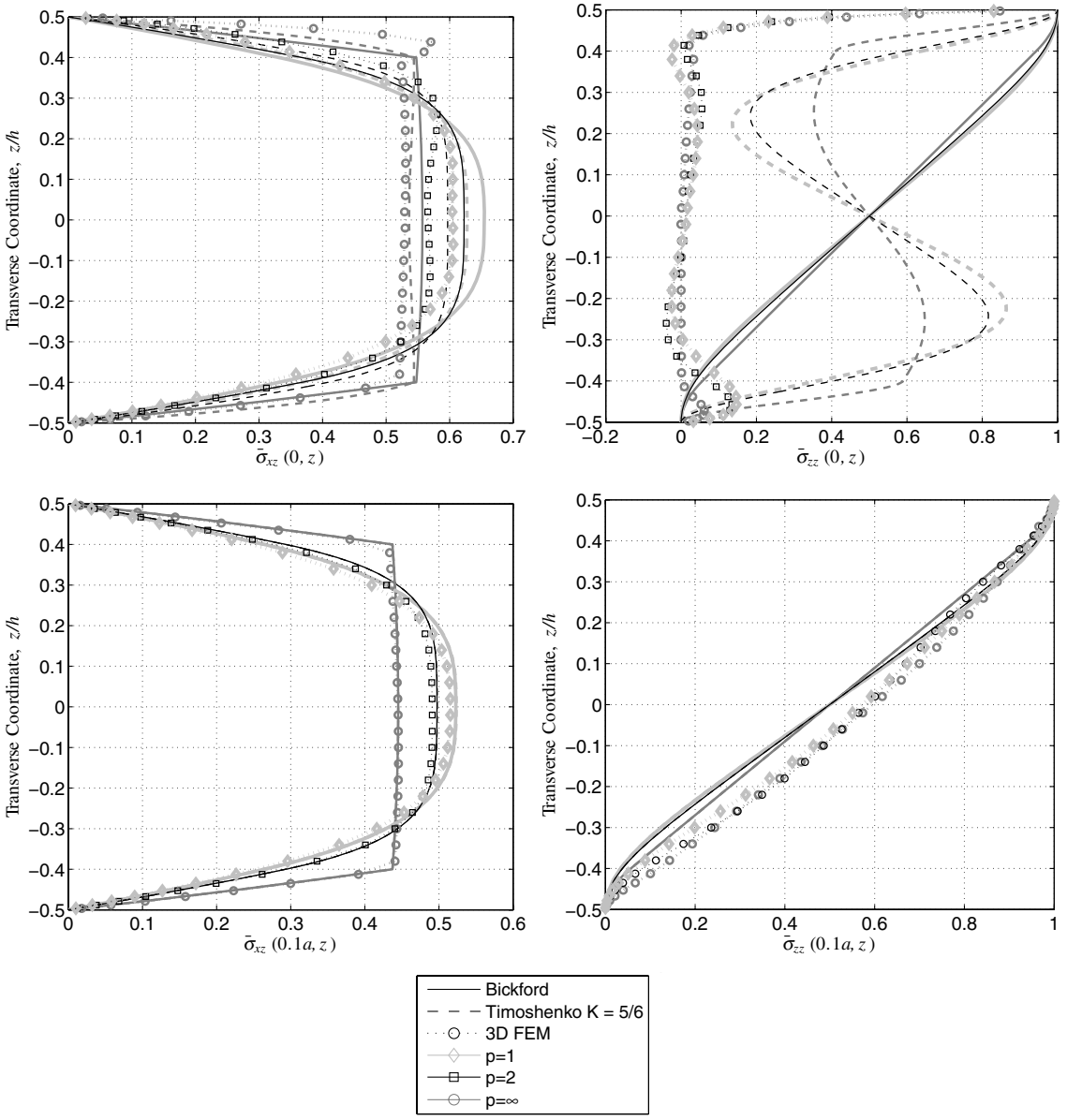

Fig. 12 Transverse shear and transverse normal stress components at $x = 0, 0.1a$ for a functionally graded sandwich beam with $p = 1, 2, 4, \infty$.

$E = 7.0 \times 10^8$ N/m^2 and $\nu = 0.3$ for the core material. The Mori–Tanaka homogenization technique was used to determine the equivalent stiffnesses at a point. The geometry was kept constant for each material variation ($a/h = 10$, $a/b = 10$, and $t_f/h = 0.1$).

Eight-node linear reduced-integration brick elements (C3-D8R) in ABAQUS/Standard were used to obtain an approximate 3-D elasticity solution for each material variation. We reduced the element size until we obtained a similar solution from two successively fine meshes. The converged mesh sizes are summarized in Table 2. The simply supported boundary condition was enforced at both edges in the same manner as for the laminated beams.

The present results were obtained using the SIHD implemented in MATLAB. As for laminated beams, we used $N = 100$ (201 sinc points) in the original sinc approximation in Eq. (2). The sinc mesh size h was taken to be $2.5/N$. The transverse normal and transverse shear stress components were obtained using numerical indefinite integration by double-exponential transformation implemented in MATLAB.

For $p = 1, 2,$ and ∞, through-the-thickness stress distributions are plotted in Figs. 11 and 12. The longitudinal normal stress σ_{xx} is plotted at the midpoint of the beam in Fig. 11. The figure indicates that the stress distribution is very accurately predicted by both ESL theories for all material variations. The stress is very accurately predicted through the functionally graded core. The transverse normal stress σ_{zz} is also plotted at the midpoint of the beam. The figure indicates that although neither ESL theory precisely captures the stress distribution, both approximate the trend quite well.

In Fig. 12, we plotted through-the-thickness stress distributions of transverse shear σ_{xz} and transverse normal σ_{zz} stresses at the end ($x/a = 0$) and near the end ($x/a = 0.1$) of the beam. The results are similar to the laminated beams in that both stress components are inaccurate at $x/a = 0$; however, at $x/a = 0.1$, the stresses very accurately approximate the stress distribution of 3-D FEM. Note that the transverse shear stress component σ_{xz} is very closely approximated for all p at $x/a = 0.1$. This indicates the success with which the integration is performed using the double-exponential integration, yet it is at little additional computation expense because the integration weights are retained from SIHD.

VI. Conclusions

Computation of transverse shear and transverse normal stresses or interlaminar stresses from 1-D ESL beam theories using the sinc method based on interpolation of the highest derivative (SIHD) [11] is performed. We obtain stresses in simply supported symmetric cross-ply laminated beams and simply supported sandwich composite beams with functionally graded cores using SIHD to approximately solve the static governing equations of the

Timoshenko beam theory and the Bickford consistent-higher-order beam theory. Integration of the equilibrium equations of elasticity is performed to obtain the transverse normal and transverse shear stress components. For the sandwich composites, we use numerical indefinite integration by the double-exponential transformation to approximate the transverse shear and transverse normal stresses. Our present numerical results obtained by SIHD were compared with an approximate elasticity solution using the 3-D FEM. Our results indicate that the stress may be accurately found from the ESL theories throughout the majority of the domain. However, near the ends of the beam, the present results differ significantly from the FEM results because of edge effects not captured by the 1-D analysis.

Appendix: Governing Equations of ESL Beam Theories

Governing equations for the beam theories are derived from the principle of virtual work: that is,

$$\int_{\Omega}[\sigma_{xx}\delta\epsilon_{xx}+\sigma_{xz}\delta\gamma_{xz}]\mathrm{d}V=\int_{\partial\Omega}f_z\delta w\mathrm{d}A \tag{A1}$$

where f_z is the bending surface traction. After some math, we obtain the governing equations for a symmetrically laminated Bickford beam theory to be

$$\frac{d\bar{Q}_x}{dx}+c_1\frac{d^2P_{xx}}{dx^2}+q=0,\qquad \frac{d\bar{M}_{xx}}{dx}-\bar{Q}_x=0$$

where Q_x, R_x, and P_{xx} were defined in Eq. (10); $\bar{Q}_x=Q_x-3c_1R_x$; $\bar{M}_{xx}=M_{xx}-c_1P_{xx}$;$c_1=4/3h^2$; and $q=bf_z$ for a rectangular cross section.

The primary variables are w_0, dw_0/dx, and ϕ_x. The corresponding secondary variables are V_x, P_{xx}, and $\bar{M}_{xx}$, where $V_x=c_1dP_{xx}/dx+\bar{Q}_x$. If we substitute the stress-resultant strain relation given by Eq. (11) and the strain definition equation (13), and if we simplify, we obtain

$$T_1\frac{d\phi_x}{dx}+T_2\frac{d^2w_0}{dx^2}+T_3\frac{d^4w_0}{dx^4}=-q$$
$$T_4\phi_x+T_5\frac{d^2\phi_x}{dx^2}+T_6\frac{dw_0}{dx}+T_7\frac{d^3w_0}{dx^3}=0$$

where

$$T_1=\frac{c_1(D^*_{11}-c_1F^*_{11})\bar{A}S^*_{55}}{\bar{D}^*_{11}},\qquad T_2=T_1$$
$$T_3=\frac{c_1^2(F^{*2}_{11}-D^*_{11}H^*_{11})}{\bar{D}^*_{11}},\qquad T_4=-\bar{A}S^*_{55},\qquad T_5=\bar{D}^*_{11}$$
$$T_6=T_4,\qquad T_7=c_1^2H^*_{11}-c_1F^*_{11}$$
$$\bar{A}S^*_{55}=AS^*_{55}-6c_1DS^*_{55}+9c_1^2FS^*_{55}$$
$$\bar{D}^*_{11}=D^*_{11}-2c_1F^*_{11}+c_1^2H^*_{11}$$

The boundary conditions at a simply supported end corresponding to $x=x_0$ are $w_0(x_0)=0$, $\bar{M}_{xx}(x_0)=0$, and $P_{xx}(x_0)=0$.

Solving the Bickford Beam Problem Using SIHD

An approximate solution may be obtained for a Bickford beam using SIHD. First, we select $n=2N+1$ collocation points on $\xi\in(0,1)$ by the DE transformation. For a mesh size h, we select collocation points corresponding to $j=\{-N,-N+1,\ldots,N-1,N\}$ by $\xi_j=\psi(jh)$ [see Eq. (1)].

The domain $x\in[0,L]$ is transformed to $\xi\in(\xi_{-N},\xi_N)$ by the linear transformation

$$\xi=\frac{x(\xi_N-\xi_{-N})}{L}+\xi_{-N} \tag{A2}$$

Accordingly, our governing equations become

$$T_1\frac{d\phi_x(x(\xi))}{d\xi}\frac{d\xi}{dx}+T_2\frac{d^2w_0(x(\xi))}{d\xi^2}\left(\frac{d\xi}{dx}\right)^2+T_3\frac{d^4w_0(x(\xi))}{d\xi^4}\left(\frac{d\xi}{dx}\right)^4=-q$$
$$T_4\phi_x(x(\xi))+T_5\frac{d^2\phi_x(x(\xi))}{d\xi^2}\left(\frac{d\xi}{dx}\right)^2+T_6\frac{dw_0(x(\xi))}{d\xi}\frac{d\xi}{dx}+T_7\frac{d^3w_0(x(\xi))}{d\xi^3}\left(\frac{d\xi}{dx}\right)^3=0$$

Assuming $d^4w_0(x(\xi_j))/d\xi^4$ and $d^2\phi_x(x(\xi_j))/d\xi^2$ are known for $j=\{-N,-N+1,\ldots,N-1,N\}$, we may then write the lower derivatives and primary functions employing the double-exponential integration scheme. We may say

$$\frac{d^3w_0(x(\xi_i))}{d\xi^3}=k_{ij}\frac{d^4w_0(x(\xi_j))}{d\xi^4}+C_0$$
$$\frac{d^2w_0(x(\xi_i))}{d\xi^2}=k_{il}k_{lj}\frac{d^4w_0(x(\xi_j))}{d\xi^4}+C_0\xi_i+C_1$$
$$\frac{dw_0(x(\xi_i))}{d\xi}=k_{im}k_{ml}k_{lj}\frac{d^4w_0(x(\xi_j))}{d\xi^4}+\frac{C_0\xi_i^2}{2}+C_1\xi_i+C_2$$
$$w_0(x(\xi_i))=k_{in}k_{nm}k_{ml}k_{lj}\frac{d^4w_0(x(\xi_j))}{d\xi^4}+\frac{C_0\xi_i^3}{6}+\frac{C_1\xi_i^2}{2}+C_2\xi_i+C_3$$
$$\frac{d\phi_x(x(\xi_i))}{d\xi}=k_{ij}\frac{d^2\phi_x(x(\xi_j))}{d\xi^2}+C_4$$
$$\phi_x(x(\xi_i))=k_{il}k_{lj}\frac{d^2\phi_x(x(\xi_j))}{d\xi^2}+C_4\xi_i+C_5$$

Now let $\{u\}=\{C_0,C_2,C_3,C_4,C_5,\{w^{(iv)}_{-N,N}\},\{\phi''_{-N,N}\}\}^T$ be the $(2n+6)\times1$ global unknown vector, where $\{w^{(iv)}_{-N,N}\}$ and $\{\phi''_{-N,N}\}$ are $n\times1$ vectors of the respective variable derivatives at each of the n sinc points. Furthermore, we say

$$[E_1]=[0_{6\times n},I_n,0_{n\times n}],\qquad [A_1]=[1_{n\times1},0_{n\times5},k_{ij},0_{n\times n}]$$
$$[B_1]=[\xi_i,1_{n\times1},0_{n\times4},g_{ij},0_{n\times n}]$$
$$[C_1]=[\xi_i^2/2,\xi_i,1_{n\times1},0_{n\times3},f_{ij},0_{n\times n}]$$
$$[D_1]=[\xi_i^3/6,\xi_i^2/2,\xi_i,1_{n\times1},0_{n\times2},e_{ij},0_{n\times n}]$$
$$[E_2]=[0_{6\times n},0_{n\times n},I_n],\qquad [A_2]=[0_{n\times4},1_{n\times1},0_{n\times1},0_{n\times n},k_{ij}]$$
$$[B_2]=[0_{n\times4},\xi_i,1_{n\times1},0_{n\times n},g_{ij}]$$

where k_{ij} is the $n\times n$ submatrix of integration weights as computed from Eq. (5), $g_{ij}=k_{il}k_{lj}$ is $n\times n$, $f_{ij}=k_{im}k_{ml}k_{lj}$ is $n\times n$, $e_{ij}=k_{in}k_{nm}k_{ml}k_{lj}$ is $n\times n$, ξ_i is an $n\times1$ submatrix of sinc points, I_n is the $n\times n$ identity matrix with submatrices of zeros and ones with indicated dimensions. Note that $[E_1]$, $[E_2]$, $[A_1]$, $[A_2]$, $[B_1]$, $[B_2]$, $[C_1]$, and $[D_1]$ each have dimensions of $n\times(2n+6)$.

With the preceding definitions, we can express the highest-order derivatives, the lowest-order derivatives, and the unknown functions w and ϕ_x in terms of a linear expression for the global unknown $\{u\}$. We may say

$$\left\{w^{(iv)}_{-N,N}\right\}^T=[E_1]\{u\},\qquad \left\{w'''_{-N,N}\right\}^T=[A_1]\{u\}$$
$$\left\{w''_{-N,N}\right\}^T=[B_1]\{u\},\qquad \left\{w'_{-N,N}\right\}^T=[C_1]\{u\}$$
$$\{w_{-N,N}\}^T=[D_1]\{u\},\qquad \left\{\phi''_{-N,N}\right\}^T=[E_2]\{u\}$$
$$\{\phi'_{-N,N}\}^T=[A_2]\{u\},\quad \text{and}\quad \{\phi_{-N,N}\}^T=[B_2]\{u\} \tag{A3}$$

where $\{w_{-N,N}\}$, $\{w'_{-N,N}\}$, $\{w''_{-N,N}\}$, $\{w'''_{-N,N}\}$, $\{\phi_{-N,N}\}$, and $\{\phi'_{-N,N}\}$ are $1 \times n$ row matrices of the respective variable derivative at each of the n sinc points. Note that prime indicates differentiation with respect ξ and not with respect to x. To obtain derivatives with respect to x, we must multiply by the appropriate power of $d\xi/dx$.

We will satisfy the governing equations at each sinc point by imposing

$$\left[T_1[A_2]\frac{d\xi}{dx} + T_2[B_1]\left(\frac{d\xi}{dx}\right)^2 + T_3[E_1]\left(\frac{d\xi}{dx}\right)^4\right]\{u\} = -\{q\}$$
$$\left[T_4[B_2] + T_5[E_2]\left(\frac{d\xi}{dx}\right)^2 + T_6[C_1]\frac{d\xi}{dx} + T_7[A_1]\left(\frac{d\xi}{dx}\right)^3\right]\{u\} = 0_{1\times n} \tag{A4}$$

where

$$\{q\} = \{q(x(\xi_{-N})), q(x(\xi_{-N+1})), \ldots, q(x(\xi_{N-1})), q(x(\xi_N))\}^T$$

The natural and essential boundary conditions are imposed in a slightly modified manner from Li and Wu's [11] SIHD. For the details of this modification, we refer the readers to Slemp and Kapania [13]. The boundary conditions are imposed at the sinc points ξ_{-N} and ξ_N. For the simply supported case, we impose $w_0(x) = 0$, $\bar{M}_{xx}(x) = 0$,, and $P_{xx}(x) = 0$ for $x = x(\xi_{-N}) = 0$ and $x = x(\xi_N) = L$. If we let $\{l_0\} = \{1, 0_{1\times(n-1)}\}$ and $\{l_L\} = \{0_{1\times(n-1)}, 1\}$, then we can write the boundary conditions in terms of the global unknown vector $\{u\}$: that is,

$$w_0(0)\text{: } \{l_0\}[D_1]\{u\} = 0$$
$$\bar{M}_{xx}(0)\text{: } \{l_0\}\left[\bar{D}^*_{11}[A_2]\frac{d\xi}{dx} + (c_1^2 H^*_{11} - c_1 F_{11})[B_1]\left(\frac{d\xi}{dx}\right)^2\right]\{u\} = 0$$
$$P_{xx}(0)\text{: } \{l_0\}\left[F^*_{11}[A_2]\frac{d\xi}{dx} - c_1 H^*_{11}\left([A_2]\frac{d\xi}{dx} + [B_1]\left(\frac{d\xi}{dx}\right)^2\right)\right]\{u\} = 0$$
$$w_0(L)\text{: } \{l_L\}[D_1]\{u\} = 0$$
$$\bar{M}_{xx}(L)\text{: } \{l_L\}\left[\bar{D}^*_{11}[A_2]\frac{d\xi}{dx} + (c_1^2 H^*_{11} - c_1 F_{11})[B_1]\left(\frac{d\xi}{dx}\right)^2\right]\{u\} = 0$$
$$P_{xx}(L)\text{: } \{l_L\}\left[F^*_{11}[A_2]\frac{d\xi}{dx} - c_1 H^*_{11}\left([A_2]\frac{d\xi}{dx} + [B_1]\left(\frac{d\xi}{dx}\right)^2\right)\right]\{u\} = 0 \tag{A5}$$

We can express the complete system of $2n + 6$ equations by Eqs. (A4) and (A5). Solving for $\{u\}$, we obtain the highest-order derivatives, the lowest-order derivatives, and the primary function at each of the sinc points by Eq. (A3). We can interpolate between the sinc points using a sinc series such as Eq. (2) or any other mechanism for interpolation. The ease with which the higher-order derivatives are computed makes SIHD an attractive tool for interlaminar stress computation.

Acknowledgments

We would like to thank the U.S. Department of Defense and the U.S. Army Research Office for funding the National Defense Science and Engineering Graduate (NDSEG) Fellowship that supported this work.

References

[1] Kapania, R. K., and Raciti, S., "Recent Advances in Analysis of Laminated Beams and Plates, Part 1: Shear Effects and Buckling," *AIAA Journal*, Vol. 27, No. 7, 1989, pp. 923–935. doi:10.2514/3.10202

[2] Kant, T., and Swaminathan, K., "Estimation of Transverse/Interlaminar Stresses in Laminated Composites—A Selective Review and Survey of Current Developments," *Composite Structures*, Vol. 49, No. 1, 2000, pp. 65–75. doi:10.1016/S0263-8223(99)00126-9

[3] Pagano, N., "Exact Solution for Composite Laminates in Cylindrical Bending," *Journal of Composite Materials*, Vol. 3, No. 3, 1969, pp. 398–411. doi:10.1177/002199836900300304

[4] Kim, J. Y., and Hong, C. S., "Three-Dimensional Finite Element Analysis of Interlaminar Stresses in Thick Composite Laminates," *Computers and Structures*, Vol. 40, No. 6, 1991, pp. 1395–1404. doi:10.1016/0045-7949(91)90410-N

[5] Phan, N. D., and Reddy, J. N., "Analysis of Laminated Composite Plates Using a Higher-Order Shear Deformation Theory," *International Journal for Numerical Methods in Engineering*, Vol. 21, No. 12, 1985, pp. 2201–2219. doi:10.1002/nme.1620211207

[6] Lajczok, M. R., "New Approach in the Determination of Interlaminar Shear Stresses from the Results of MSC/NASTRAN," *Computers and Structures*, Vol. 24, No. 4, 1986, pp. 651–656. doi:10.1016/0045-7949(86)90204-X

[7] Byun, C., and Kapania, R. K., "Prediction of Interlaminar Stresses in Laminated Plates Using Global Orthogonal Interpolation Polynomials," *AIAA Journal*, Vol. 30, No. 11, 1992, pp. 2740–2749. doi:10.2514/3.11293

[8] Lee, K., and Lee, S. W., "A Postprocessing Approach to Determine Transverse Stresses in Geometrically Nonlinear Composite and Sandwich Structures," *Journal of Composite Materials*, Vol. 37, No. 24, 2003, pp. 2207–2224. doi:10.1177/0021998303038111

[9] Roos, R., Kress, G., and Ermanni, P., "A Post-Processing Method for Interlaminar Normal Stresses in Doubly Curved Laminates," *Composite Structures*, Vol. 81, No. 3, 2007, pp. 463–470. doi:10.1016/j.compstruct.2006.09.016

[10] Noor, A., and Malik, M., "Accurate Determination of Transverse Normal Stresses in Sandwich Panels Subjected to Thermomechanical Loadings," *Computer Methods in Applied Mechanics and Engineering*, Vol. 178, Nos. 3–4, 1999, pp. 431–443. doi:10.1016/S0045-7825(99)00025-0

[11] Li, C., and Wu, X., "Numerical Solution of Dierential Equations Using the Sinc Method Based on the Interpolation of the Highest Derivatives," *Applied Mathematical Modeling*, Vol. 31, No. 1, 2007, pp. 1–9.

[12] Bickford, W. B., "A Consistent Higher Order Beam Theory," *Developments in Theoretical and Applied Mechanics*, Vol. 11, Dept. of Mechanical Engineering, Univ. of Alabama in Huntsville, Huntsville, AL, Apr. 1982, pp. 137–150.

[13] Slemp, W. C. H., and Kapania, R. K., "Imposing Boundary Conditions in Sinc Method Using Highest Derivative Approximation," *Journal of Computational and Applied Mathematics* (submitted for publication); also 9th U.S. National Congress on Computational Mechanics, San Francisco, U.S. Association for Computational Mechanics Paper 016-5, July 2007.

[14] Muhammad, M., and Mori, M., "Double Exponential Formulas for Numerical Indenite Integration," *Journal of Computational and Applied Mathematics*, Vol. 161, No. 2, 2003, pp. 431–448. doi:10.1016/j.cam.2003.05.002

[15] Muhammad, M., Nurmuhammad, A., Mori, M., and Sugihara, M., "Numerical Solution of Integral Equations by Means of the Sinc Collocation Method Based on the Double Exponential Transformation," *Journal of Computational and Applied Mathematics*, Vol. 177, No. 2, 2005, pp. 269–286. doi:10.1016/j.cam.2004.09.019

[16] Mori, M., "Discovery of the Double Exponential Transformation and its Developments," *Publications of the Research Institute for Mathematical Sciences*, Vol. 41, No. 4, 2005, pp. 897–935; also available online at http://www.kurims.kyoto-u.ac.jp/~okamoto/paper/Publ_RIMS_DE/41-4-38.pdf.

[17] Mori, M., and Sugihara, M., "The Double-Exponential Transformation in Numerical Analysis," *Journal of Computational and Applied Mathematics*, Vol. 127, No. 1, 2001, pp. 287–296. doi:10.1016/S0377-0427(00)00501-X

[18] Takahasi, H., and Mori, M., "Double Exponential Formulas for Numerical Integration," *Publications of the Research Institute for Mathematical Sciences*, Vol. 9, No. 3, 1974, pp. 721–741.

[19] Sugihara, M., and Matsuo, T., "Recent Developments of the Sinc Numerical Methods," *Journal of Computational and Applied Mathematics*, Vols. 164–165, No. 1, 2004, pp. 673–689. doi:10.1016/j.cam.2003.09.016

[20] Abramowitz, M., and Stegun, I. A. (eds.), *Handbook of Mathematical Functions with Formulas, Graphs, and Mathematical Tables*, 9th printing, Dover, New York, 1972.

[21] Reddy, J. N., *Mechanics of Laminated Composite Plates—Theory and Analysis*, CRC Press, Boca Raton, FL, 2004.

[22] Goyal, V. K., and Kapania, R. K., "A Shear-Deformable Beam Element for the Analysis of Laminated Composites," *Finite Elements in Analysis and Design*, Vol. 43, No. 6, 2007, pp. 463–477. doi:10.1016/j.finel.2006.11.011

[23] Mori, T., and Tanaka, K., "Average Stress in Matrix and Average Elastic Energy of Materials with Misting Inclusions," *Acta Metallurgica*, Vol. 21, No. 5, 1973, pp. 571–574. doi:10.1016/0001-6160(73)90064-3

[24] Ferreira, A., Batra, R., Roque, C., Qian, L., and Martins, P., "Static Analysis of Functionally Graded Plates Using Third-Order Shear Deformation Theory and a Meshless Method," *Composite Structures*, Vol. 69, No. 4, 2005, pp. 449–457. doi:10.1016/j.compstruct.2004.08.003

[25] Ferreira, A., Batra, R., Roque, C., Qian, L., and Jorge, R., "Natural Frequencies of Functionally Graded Plates by a Meshless Method," *Composite Structures*, Vol. 75, Nos. 1–4, 2006, pp. 593–600. doi:10.1016/j.compstruct.2006.04.018

[26] Zenkour, A., "A Comprehensive Analysis of Functionally Graded Sandwich Plates: Part 1—Deection and Stresses," *International Journal of Solids and Structures*, Vol. 42, Nos. 18–19, 2005, pp. 5224–5242. doi:10.1016/j.ijsolstr.2005.02.015

A. Palazotto
Associate Editor